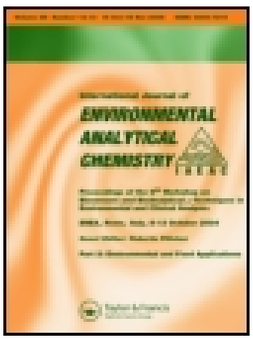

International Journal of Environmental Analytical Chemistry

ISSN: 0306-7319 (Print) 1029-0397 (Online) Journal homepage: http://www.tandfonline.com/loi/geac20

Electrochemical determination of picric acid based on platinum nanoparticles–reduced graphene oxide composite

Mojtaba Mahyari

To cite this article: Mojtaba Mahyari (2016): Electrochemical determination of picric acid based on platinum nanoparticles–reduced graphene oxide composite, International Journal of Environmental Analytical Chemistry, DOI: 10.1080/03067319.2016.1268606

To link to this article: http://dx.doi.org/10.1080/03067319.2016.1268606

Published online: 21 Dec 2016.

INTERNATIONAL JOURNAL OF ENVIRONMENTAL ANALYTICAL CHEMISTRY, 2016
http://dx.doi.org/10.1080/03067319.2016.1268606

Taylor & Francis
Taylor & Francis Group

Electrochemical determination of picric acid based on platinum nanoparticles–reduced graphene oxide composite

Mojtaba Mahyari

Elites Advanced Research Center, Malek-Ashtar University of Technology, Tehran, Iran

ABSTRACT

Platinum nanoparticles–reduced graphene oxide composite-modified glassy carbon electrode (PtNPs–rGO/GCE) was developed as a simple, selective and sensitive electrochemical sensor for determination of picric acid (PA). Cyclic voltammogram (CV) of PA showed three well-defined irreversible reduction peaks at the potentials of −0.43, −0.57 and −0.66 V versus Ag/AgCl. In this work, the interference effect of other nitrophenol compounds (NPhCs) was significantly reduced by appropriate adjusting of pH. Square wave voltammetry was used for quantification of PA in the range of 5–500 μM (1.15–115 mg L^{-1}) with practical detection limit of 1 μM (0.23 mg L^{-1}). The proposed sensor was successfully applied for the determination of PA in two natural water samples.

ARTICLE HISTORY
Received 25 June 2016
Accepted 29 November 2016

KEYWORDS
Electrochemical sensor; explosive sensor; picric acid; platinum nanoparticles; reduced graphene oxide

1. Introduction

Picric acid (PA) or 2,4,6-trinitrophenol (TNP), which is a member of nitrophenol compounds (NPhCs), is known as a common and very serious organic pollutant of water with very harmful effects on humans and animals [1–3]. In addition, similar to other highly nitrated compounds such as well-known trinitrotoluene (TNT), PA is a powerful explosive compound. It was used as an explosive compound and weapon until World War I [4]. However, it also has widespread applications in different fields of science and technology such as medicine (antiseptic, malaria, trichinosis, herpes and smallpox treatments), organic synthesis, projectiles (as a burster), rocket fuels, fireworks, coloured glass, batteries, disinfectants, pharmaceutical and leather industries, production of fast dyes for wool and silk, metal etching and photographic chemicals and production of laboratory reagents [5–8]. PA can also be used as a reagent in indirect analysis including determination of creatinine [9], reducing sugar determination in Port wines [10] and quantification of oxybutynin hydrochloride [11]. Consequently, the importance of monitoring PA in military, environmental and human health applications has led to an increasing demand for developing a facile, sensitive, selective and cost-efficient method for the determination of PA.

Several analytical methods have been developed for determining PA such as spectrophotometric [12], fluorescence [4,6], mass spectrometry [13], high-performance liquid chromatography [14], capillary electrophoresis [15], extraction [16] and electrochemical methods [17–21]. Compared to the above-mentioned methods, electrochemical

CONTACT Mojtaba Mahyari m_mahyari@sbu.ac.ir

techniques have advantages such as simplicity, selectivity, rapidity, low cost and easy miniaturisation [22]. So far, various PA electrochemical sensors have been developed. For instance, Vyskočil et al. introduced silver solid amalgam composite electrode for determination of PA [17]. This sensor is not environmentally friendly since it contains toxic Hg. In another report, Jaffrezic-Renault et al. used bulk bismuth electrode as an electrochemical sensor for determination of PA [18]. However, their results did not show good selectivity. Jiarui et al. reported PA determination using a reduced graphene oxide sensor modified with 1-pyrenebutyl-amino-β-cyclodextrin [19]. The electrode was fabricated through complex multiple steps. Therefore, there is still a demand for fabrication of simple electrochemical PA sensors with improved sensitivity and selectivity.

Their unique conductivities, electrocatalytic activities, electronic properties and high corrosion resistance make redox-active metal nanoparticles (MNPs) attractive for potential applications in electrochemical nanosensors. Particularly, platinum nanoparticles (PtNPs) have been widely used as modifiers in different electrochemical nanosensors [23] because they have such benefits as high effective surface area, excellent electrocatalytic activities and efficient mass transport [24].

Recently, graphene nanosheets (GNSs) and their derivatives as a new group of carbon nanostructures have become a hot topic of interest for their applications in making sensors due to possessing extraordinary catalytic, electrical, chemical, optical, mechanical and structural properties [25,26]. Graphene oxide (GO) is one of the derivatives of graphene and has attracted a great deal of attention in the field of nanomaterials because it can be conveniently prepared in large scales and is highly dispersible in water [27,28]. GO is a two-dimensional carbon material with several oxygen functional groups such as hydroxyl, carboxyl, epoxy and lactone groups on its basal planes and edges which make it a suitable candidate for supporting MNPs.

The integration of highly conductive GNSs (or their derivatives) and MNPs leads to GNS-MNP composites forming a new way to develop electron transportation and catalytic properties [29]. Therefore, GNS-MNP composites are vastly used as a modifier in the electrochemical sensors for determining various analytes. Meilin Liu and co-workers used PtNPs-decorated three-dimensional nitrogen-doped porous graphene composite as an unprecedented electrocatalyst for methanol oxidation [30]. Zhanjun Yang and co-workers used PtNPs-functionalised nitrogen graphene nanocomposite as a suitable support for immobilising glucose oxidase and used it as a high-sensitive glucose biosensor. The PtNPs-functionalised nitrogen graphene nanocomposite provided a desirable surface for immobilising enzyme and improved the electron transfer between the enzyme and surface of the electrode [31]. Engin Er and co-workers introduced GNSs decorated with PtNPs as a high-efficient electrocatalyst for metoprolol sensing. Moreover, GNSs decorated with PtNPs enhanced the sensitivity of the electrochemical sensor by adsorption of metoprolol [32]. Shen-Ming Chen and co-workers used PtNPs–reduced graphene oxide composite (PtNPs–rGO) as an excellent electrocatalyst towards the reduction of H_2O_2 [33]. Rajendra N. Goyal and co-workers used an electrochemically rGO grafted with hybrid nanocomposite of PtNPs and Nafion as an electrocatalyst to determine of efavirenz [34]. It electrocatalyses the reaction kinetics and significantly increases the current response and reduces the oxidation peak potential of efavirenz.

In the present work, the advantages of electrocatalytic activities of PtNPs as well as the structural properties of GO were combined to modify glassy carbon electrodes. The composite was synthesised according to a non-toxic, rapid, one-pot and template-free method reported in the literature [35]. Therefore, PtNPs–rGO by which the glassy carbon electrode was modified (PtNPs–rGO/GCE) was used as a simple, selective and sensitive electrochemical sensor for the determination of PA. All the experimental parameters especially pH were optimised to achieve significant analytical figures of merit and to improve selectivity for the determination of PA. To the best of our knowledge, this is the first report on electrochemical determination of PA based on MNPs–rGO composite.

2. Experimental

2.1. *Reagents*

Graphite powders (particle size <100 µM, purity 99.9%) were purchased from Fluka. PA, 2-nitrophenol, 4-nitrophenol, 2,4-dinitrophenol, acetic acid, phosphoric acid, boric acid, sodium citrate, sodium borohydride, ethanol and NaOH were obtained from Merck. Hexachloro-platinic (IV) acid hexahydrate ($H_2PtCl_6.6H_2O$, ~40% Pt) was obtained from Sigma-Aldrich. All other reagents were of analytical grade and were used without further purification. All of the solutions were prepared in deionised distilled water. The Britton–Robinson buffer (BRB) was used as a supporting electrolyte. It was prepared by 0.1 M solution of acetic acid, phosphoric acid and boric acid and the pH was adjusted by using NaOH.

2.2. *Apparatus*

All the electrochemical measurements including cyclic voltammetry and linear sweep voltammetry and square wave voltammetry (SWV) were carried out on an Autolab electrochemical system (Eco-Chemie,Utrecht, The Netherlands) equipped with PGSTAT-12 and GPES softwares (Eco-Chemie) and a standard three-electrode cell including Ag/AgCl as the reference electrode, a platinum wire as the auxiliary electrode and bare and modified glassy carbon electrodes (GCE with 2 mm diameter from Metrohm) as working electrodes. Philips XL30 with an accelerating voltage of 25 kV was used to obtain Field Emission Scanning Electron Microscopy (FESEM) images. A Metrohm pH metre (model 780) with a combined pH glass electrode was used for pH measurements. The pH metre was calibrated against standard buffer solutions at pHs of 9.0, 7.0 and 4.0.

2.3. *Preparation of PtNPs–rGO*

GO was synthesised from a commercially available natural graphite powder by a modified Hummers method [36]. Briefly, 1.0 g of graphite powder and 1.0 g sodium nitrate were added to a 46 mL concentrated sulfuric acid kept in an ice bath and then stirred for 4 h. Then, 6.0 g of potassium permanganate was added gradually to the mixture. The rate of addition was controlled carefully to prevent the temperature of the mixture from exceeding 20°C. After that, the ice bath was removed and the mixture was stirred for 2 h at room temperature. After adding 92 mL of deionised water, the

suspension was heated for 15 min at 98°C. The mixture was then further diluted with 200 mL deionised water and treated with 20 mL hydrogen peroxide (30%). The mixture was filtered and washed with 5% HCl and then washed repeatedly with deionised water until neutral pH was obtained. The GO powder was obtained through drying at 50°C in a vacuum oven for 24 h.

The PtNPs–rGO was synthesised as described previously [35]. Briefly, a completely homogeneous and stable suspension of GO sheets in deionised water (40 mL, 1 mg mL^{-1}) was obtained by ultrasonic treatment for 15 min. Subsequently, 2 mL of 1% solution of $H_2PtCl_6.6H_2O$ was added to the GO suspension (40 mL, 1 mg mL^{-1}) and the mixture was stirred for 30 min in order to obtain a homogeneous suspension. Finally, 2 mL 1% sodium citrate, 5 mL ethanol and 1 mL 1% sodium borohydride were added to the suspension of GO and $H_2PtCl_6.6H_2O$. Then, the mixture was kept stirring for 12 h. The synthesised PtNPs–rGO composite was collected by centrifuging the resultant mixture at 12,000 rpm and washed three times by deionised water and dried in a vacuum oven at 60°C. The same procedure without adding $H_2PtCl_6.6H_2O$ was used to prepare rGO.

2.4. *Fabrication of PtNPs–rGO/GCE*

Prior to using GCE as bare or modified electrodes, it was polished with 0.3 and 0.05 µM aluminium oxide (Al_2O_3) powder and was successively ultrasonicated in ethanol and ultrapure water for 2 min. The PtNPs–rGO/GCE and rGO/GCE were prepared by dropwise adding of 6 µL of the 1 mg mL^{-1} PtNPs–rGO and rGO suspensions to the GCE surface which were then left to dry under ambient conditions. After fabricating each electrode to get a stable and reproducible response, cyclic voltammetry was performed at scan rate of 50.0 mV s^{-1} between 0.0 and −1.0 V for three times in the 0.1 mol L^{-1} BRB (pH = 6.0).

3. Results and discussion

3.1. *Characterisation of rGO and PtNPs–rGO*

The UV–Vis spectroscopy was used as the most common and most important method for showing the GO reduction [37]. The UV–Vis absorption peak position of GO is a characteristic of the degree of deoxygenation (reduction) [37]. The optical absorption spectra of the GO, rGO and PtNPs–rGO suspensions are shown in Figure 1A. After reduction of the GO the colour of the GO suspension changed from light brown to black (see the inset of Figure 1A). The absorption peak of GO was around 244 nm, while the absorption peaks of rGO shifted into wavelengths of around 271 nm. This red shift corresponds to deoxygenation of the GO suspension under the reduction process [37,38].

The functional groups on GO, rGO and PtNPs–rGO are monitored in the Fourier Transform-Infrared Spectroscopy (FT-IR) spectra (Figure 1B). The characteristic bands of O–H stretching at 3468 cm^{-1} are observed in GO, rGO and PtNPs–rGO. Furthermore, additional O–H groups are observed for GO at 3600 cm^{-1} as shoulder. The peaks which appeared at 1076, 1395, 1623 and 1735 cm^{-1} are attributed to C–O, O–H, C=C and C=O functional groups, respectively [37,39,40]. Deoxygenation of the GO after reduction

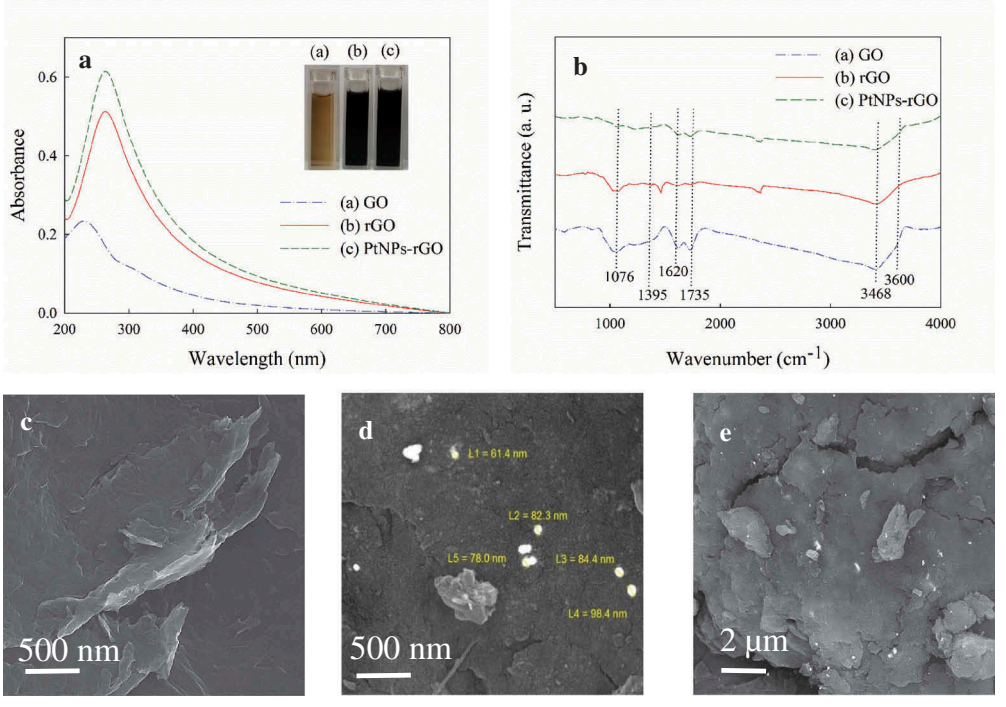

Figure 1. (A) UV–vis absorption spectra of (a) GO, (b) rGO and (c) PtNPs–rGO suspensions (0.01 mg mL^{-1}). Inset shows photographs of (a) GO, (b) rGO and (c) PtNPs–rGO suspensions (0. 1 mg mL^{-1}). (B) FTIR spectra of (a) GO, (b) rGO and (c) PtNPs–rGO. (C-D) the FESEM images of (C) rGO and (D, E) PtNPs–rGO at different magnitudes.

process is confirmed by reduction of peaks for oxygen functional groups in rGO and PtNPs–rGO.

The PtNPs–rGO was synthesised according to a previously reported procedure [35]. The structure and morphology of PtNPs–rGO has been studied by FESEM. The FESEM images of rGO and PtNPs–rGO are shown in Figure 1. As can be seen, PtNPs were observed as distinct bright nanoparticles distributed homogeneously on a large surface area of rGO sheets (Figure 1D, E). The PtNPs had an average diameter of 81 nm.

3.2. *Electrochemical behaviour of PA on PtNPs–rGO/GCE*

The electrochemical behaviour of PA was investigated by cyclic voltammetry and linear sweep voltammetry at a wide pH range of BRB solution. Some cyclic voltammograms (CVs) have been shown in Figure 2 (all peaks were subtracted from the background current). The reduction peaks of PA can be observed at all pH values ranging from 2.0 to 12.0. By increasing the solution alkalinity, the reduction peaks of PA shift towards more negative potentials. As reported previously, deprotonation of PA at a more basic medium and stabilisation of negative charge of oxygen by the nitro groups caused a more difficult reduction of PA [41].

The observation of three well-resolved PA reduction peaks (at −0.43, −0.54 and −0.66 V vs. Ag/AgCl in 0.1 M BRB pH = 6.0) is in good agreement with the reported

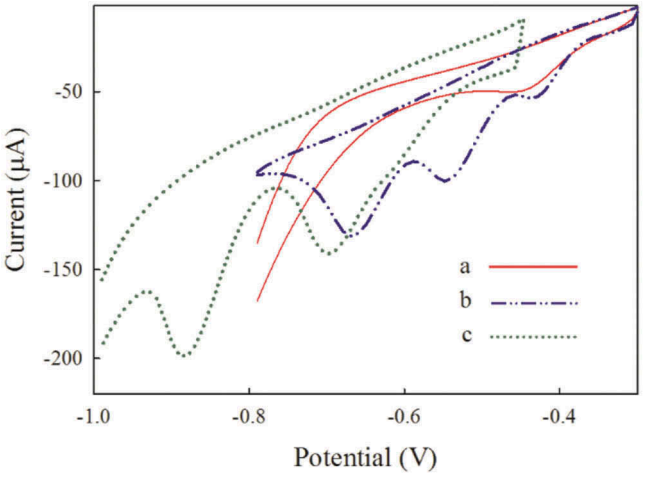

Figure 2. Cyclic voltammograms of a solution containing 1 mM PA at PtNPs–rGO/GCE in the BRB solution (0.1 M) with pH of (a) 2.0, (b) 6.0 and (c) 10.0. Scan rate: 50 mV s^{-1}. All peaks were subtracted from the background current.

mechanism in the literature. According to the reported mechanism, the reduction process of nitroaromatic compounds, such as PA, depending on the experimental conditions, can occur through several paths and one to four reduction signals can be observed [41]. The reduction of nitro group of the nitroaromatic compounds usually occurs with a multistep process (Scheme 1) [42–45]. Therefore, based on the reported mechanism, three reduction peaks of PA at pH = 6.0 are related to reductions of the PA nitro groups by the three sequential two-electron transfer steps. In the first step, nitro groups are reduced to nitroso groups by two stepwise one-electron transfers or by a two-electron transfer process (the reduction peak is at −0.43 V vs. Ag/AgCl in pH = 6.0). In the second step, the nitroso groups are reduced to hydroxylamine through a two-electron transfer process (the reduction peak is at −0.54 V vs. Ag/AgCl in pH = 6.0) and in the third step the hydroxylamine group is reduced to amine groups through a two-electron transfer process (the reduction peak is at −0.66 V vs. Ag/AgCl in pH = 6.0).

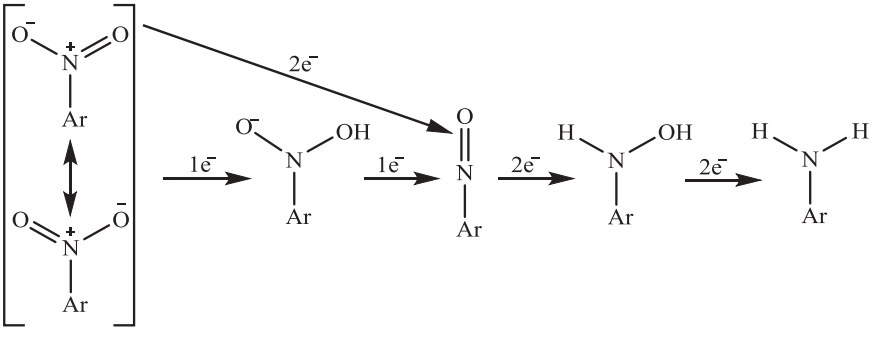

Scheme 1. Mechanism for the reduction of nitro groups in nitroaromatic compounds.

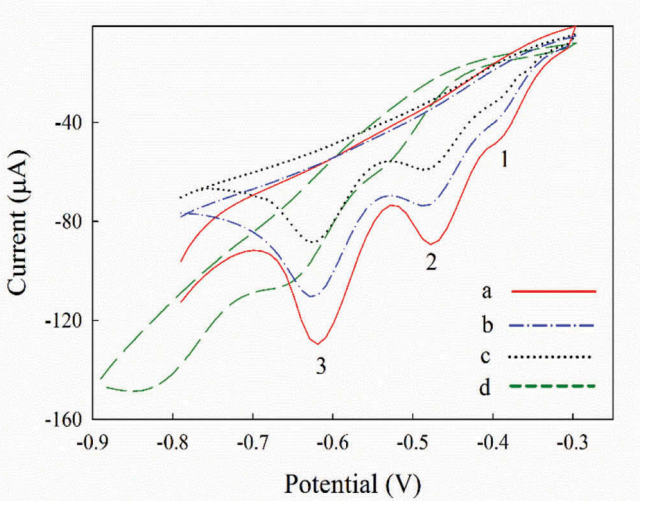

Figure 3. Cyclic voltammograms of a solution containing 1 mM PA in the BRB solution (0.1 M, pH = 6.0) at (a) PtNPs–rGO/GCE, (b) rGO/GCE, (c) GO/GCE and (d) GCE. Scan rate: 50 mV s^{-1}. All peaks were subtracted from the background current.

The electrochemical reduction of PA was compared by cyclic voltammetry at PtNPs–rGO /GCE, rGO/GCE, GO/GCE and GCE in 0.1 M BRB (pH = 5.0) at 50 mV s^{-1} (Figure 3). At this condition, three PA reduction peaks (peaks 1, 2 and 3) were observed at four different examined electrodes. As can be seen in Figure 3, the currents and potentials of the PA reduction peaks were improved significantly by modification of GCE with GO, rGO and PtNPs–rGO composites. These results confirm that GO, rGO and PtNPs have an electrocatalytic effect on the reduction of PA. In fact, the best electrocatalytic effect was observed at PtNPs–rGO/GCE. This excellent electrocatalytic activity is due to the existence of several oxygen functional groups such as hydroxyl, carboxyl, epoxy and lactone groups on the basal planes and edges of rGO [46] and also the strong accumulation of nitroaromatic compounds on the surface of nanomaterials through π-π interaction [47,48].

3.3. *Effect of pH and buffer type*

The electrochemical behaviour of organic compounds is dependent on the pH value of supporting electrolyte [49–51]. On the other hand, because of the structural similarity of the NPhCs, selectivity is one of the most important challenges for the determination of these compounds. In most of the reported electrochemical sensors, the peak potentials of the nitroaromatic compounds are very close [42,48,52]. Therefore, the pH was optimised by considering the selectivity of the sensor. Hence, the signals of three NPhCs (2-nitrophenol, 4-nitrophenol, 2, 4-dinitrophenol) that have structural similarity with PA were recorded at PtNPs–rGO/GCE in the wide pH range of BRB. Some linear sweep voltammograms have been shown in Figure 4 (all peaks were subtracted from the background current). In the whole pH range, peak 3 of the PA overlaps with reduction peaks of 4-nitrophenol and 2, 4-dinitrophenol and peak 2 of the PA overlaps

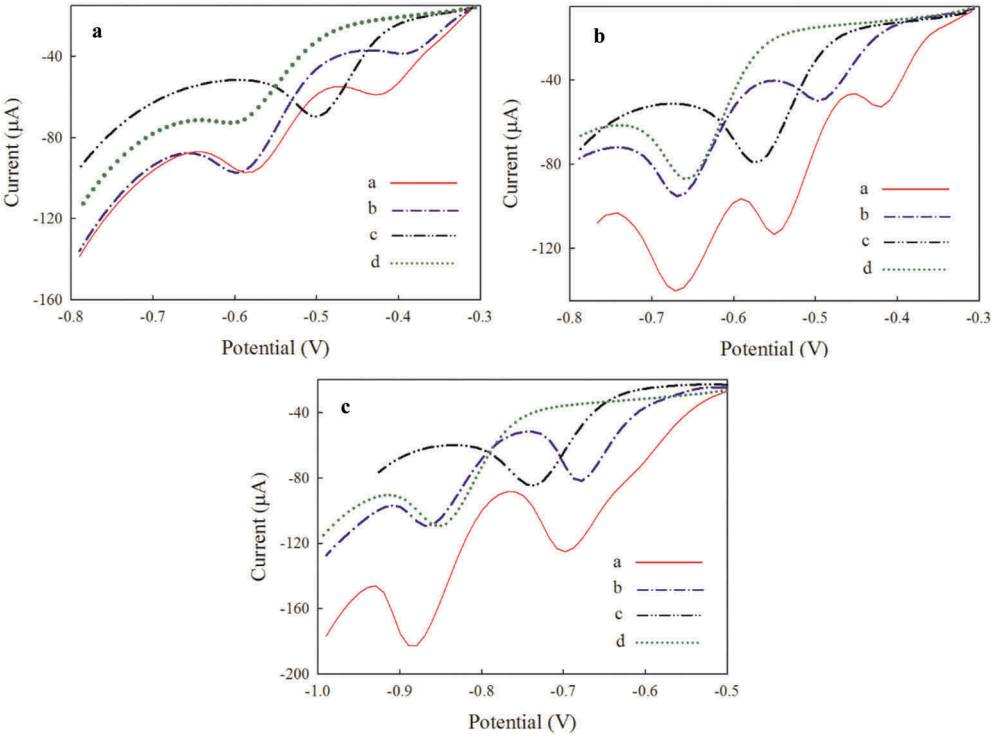

Figure 4. Linear sweep voltammograms of a solution containing 1 mM of (a) PA, (b) 2, 4nitrophenol, (c) 2 nitrophenol and (d) 4 nitrophenol at PtNPs–rGO/GCE in the BRB solution (0.1 M) pH (A) 4.0, (B) 6.0 and (C) 10.0. Scan rate: 50 mV s^{-1}. All peaks were subtracted from the background current.

with reduction peaks of 2-nitrophenol and 2, 4-dinitrophenol. Peak 1 of the PA does not show any overlap with reduction peaks of 2-nitrophenol and 4-nitrophenol in the whole pH range. Peak 1 of the PA shows an overlap with 2, 4-dinitrophenol reduction peaks at low and high pH ranges. Therefore, pH = 6.0 was selected as the optimum pH for analytical determination of PA by using peak 1 (at 0.43 V vs. Ag/AgCl) which does not have any overlap with reduction peaks of 4-nitrophenol and has a very low overlap with reduction peaks of 2-nitrophenol and 2, 4-dinitrophenol.

To investigate the effect of various buffers such as acetate buffer, citrate buffer, phosphate buffer and tris buffer as electrolyte, the analytical signals of PA (100 μM) were recorded in different buffer solutions (pH = 6.0). The results indicated that there was not a significant difference among the tested electrolytes. Hence, the BRB buffer solution (0.1 M, pH = 6.0) was selected as the electrolyte in all the experiments.

3.4. *Effect of scan rate*

Generally useful data can be acquired from potential scan rate studies such as controlling processes involved in reduction or oxidation of analytes. Hence, the effect of scan rate was investigated by recording the reduction signals of 300 μM PA solution at

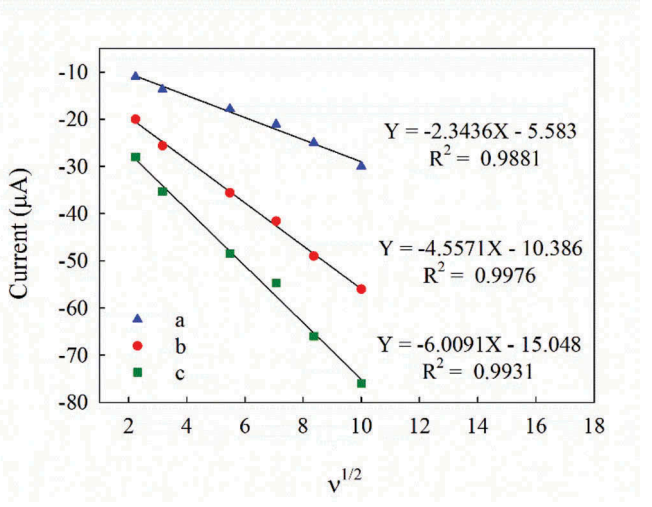

Figure 5. The plot of the currents of 300 μM PA in 0.1 M of BRB solution (pH = 6.0) versus square root of the scan rate reduction (a) peak 1, (b) peak 2 and (c) peak 3.

different scan rates ranging from 5 to 100 mV s^{-1}. As can be observed in Figure 5, the currents of the three reduction peaks of PA have a linear relation with the square root of scan rates ($v^{1/2}$) with correlation coefficients of 0.9880, 0.9976 and 0.9931 for reduction peaks of 1, 2 and 3, respectively. These results indicate that the reduction of PA at PtNPs–rGO/GCE is a diffusion-controlled process.

3.5. *Analytical figures of merit*

SWV was used in the potential range of −0.2 to −0.8 V versus Ag/AgCl for the determination of PA. The effects of SWV parameters such as pulse amplitude, frequency and scan rate on the peak current were also investigated. The optimum parameters were found to be pulse amplitude 0.05 V, frequency 10 Hz and scan rate 0.05 V s^{-1}. To indicate the linear relation between the net reduction peak currents, as analytical signals, and the concentrations of PA, standard solutions of PA were prepared in BRB (pH = 6.0). Three good linearities were obtained between the currents of three reduction peaks and the concentrations of PA in the concentration range of 5–500 μM (1.15–115 mg L^{-1}) with correlation coefficients of 0.9986, 0.9987 and 0.9974 for the reduction peaks of 1, 2 and 3, respectively (Figure 6). Calibration plots of the reduction peak currents versus concentrations of PA are presented in Figure 6. The experimental detection limit (S/N = 3) was found to be 1 μM (0.23 mg L^{-1}).

To investigate the precision of the calibration standard, five replicates of low, medium and high concentrations (70, 200 and 400 μM) of PA were used in 1 and 5 different days for intra- and inter-day precisions studies, respectively. The mean relative standard deviation (RSD %) for intra- and inter-day precisions assay were 2.83% and 3.30%, respectively. The reproducibility of the electrode signal was evaluated by analysing a solution containing 200 μM of PA with five different PtNPs–rGO/GCE electrodes and five different analysts. An excellent reproducibility was observed with the RSD % value of

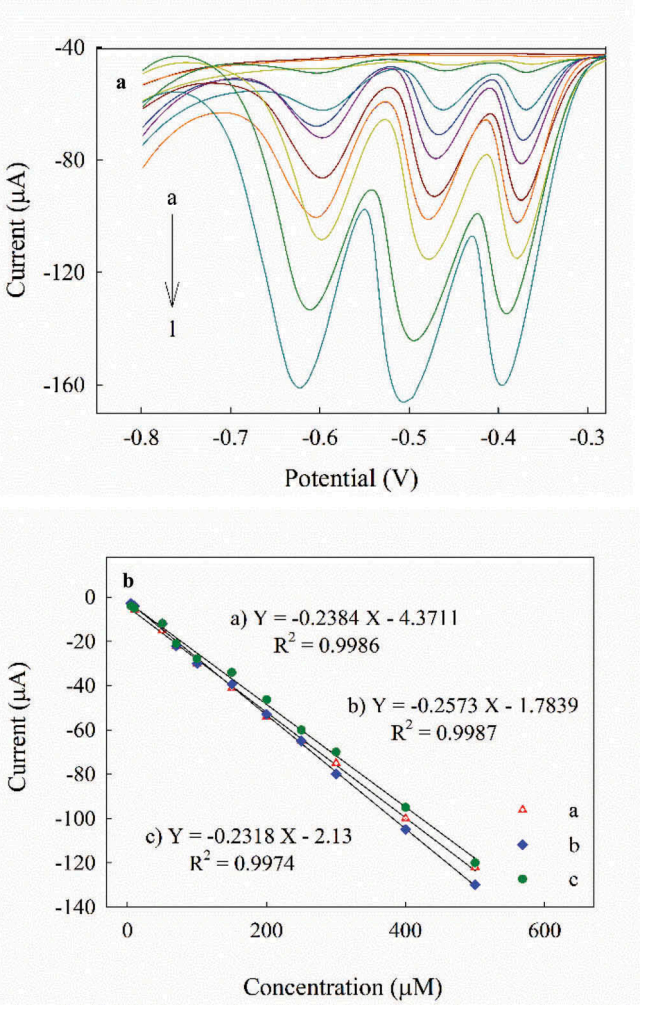

Figure 6. (A) SWV curves of different concentrations of PA in 0.1 M BRB at PtNPs–rGO/GCE: (a) blank (b) 5, (c) 10, (d) 50, (e) 70, (f) 100, (g) 150, (h) 200, (i) 250, (j) 300, (k) 400 and (l) 500 µM. Pulse amplitude = 0.05 V, frequency = 10 Hz and scan rate = 0.05 V. (B) The obtained calibration lines for PA reduction (a) peak 1, (b) peak 2 and (c) peak 3.

4.57%. All the RSD % were below 5% which means that they are acceptable for standard samples.

A comparison between the analytical figures of merit for the proposed electrode (PtNPs–rGO/GCE) and previously reported electrochemical sensors has been presented in Table 1. An excellent performance was observed for the PtNPs–rGO/GCE compared to those of most other electrochemical sensors considering linear calibration range.

3.6. *Interferences*

The selectivity of the proposed sensor was evaluated by studying the influence of various potentially interfering species in real samples on the determination of 100 µM

Table 1. A comparison of different sensors for electrochemical determination of PA.

Electrode	Linear range (μM)	Detection limit (μM)	Reference
Solid amalgam composite electrode	–	1	[17]
Bismuth electrode	2.6–30	0.8	[18]
Reduced graphene oxide modification with 1-pyrenebutyl-amino-β-cyclodextrin	5.0–215	0.52	[19]
CuS nanoparticles deposited on nitrogen-doped reduced graphene oxide	1.6–3.2	0.07	[20]
Bismuth modified microwire	–	13.1	[21]
Copper electrode	20–300	6.0	[41]
PtNPs–rGO/GCE	5–500	1	This work

PA. In this work, the pH was adjusted to decrease the interfering effect of other NPhCs, which have a structural similarity with PA on the reduction peak 1 of PA. Hence, the interference effect of variable concentrations of potentially interfering species on the reduction peak 1 of PA was recorded under optimum conditions (BRB, pH = 6.0). The maximum tolerable concentrations of potentially interfering compounds are listed in Table 2. Because of the poor solubility of some potentially interfering species in PBS solution, ethanol was used as a cosolvent to increase their solubility. The satisfactory selectivity of the proposed electrode for determination of PA was confirmed by the results in Table 2.

3.7. *Real sample analysis*

The applicability of the proposed electrode (PtNPs–rGO/GCE) for quantification of PA was assessed by determination of PA in waste and lake water samples. The real samples were characterised by a hydrological company in Shiraz, Iran. The waste water contained chloride (177.5 mg L^{-1}), sulphate (144 mg L^{-1}), nitrate (36.48 mg L^{-1}), nitrite (0.7 mg L^{-1}), phosphate (37.5 mg L^{-1}), ammonium (44.5 mg L^{-1}), detergent (0.038 mg L^{-1}), oil (28.5 mg L^{-1}), total suspended solids (54 mg L^{-1}), total organic carbon (20 mg L^{-1}) and total dissolved solids (1572 mg L^{-1}). The lake water contained chloride (142 mg L^{-1}), calcium (70 mg L^{-1}), magnesium (12 mg L^{-1}), sodium (77.28 mg L^{-1}), potassium (1.56 mg L^{-1}), sulphate (16. 8 mg L^{-1}), nitrate (1.58 mg L^{-1}), nitrite (0.004 mg L^{-1}), phosphate (0.03 mg L^{-1}), ammonium (0.4 mg L^{-1}), carbonate (7.25 mg L^{-1}), bicarbonate (213.5 mg L^{-1}), water hardness (225 mg L^{-1}), temporary hardness (175 mg L^{-1}), total organic carbon (0.9 mg L^{-1}) and total dissolved solids (533 mg L^{-1}). The real samples were analysed without any dilution or pretreatment.

Table 2. Interference study for determination of 100 μM PA*.

Species	Maximum tolerable concentration ratio
K^+, Mg^{2+}, Ca^{2+}, Fe^{2+}, Hg^{2+}, Pb^{2+}, Cu^{2+}, Ni^{2+}, SO_4^{2-}, F^-, B^-r, Cl^-, HCO_3^-, NO_3^-, Dopamine, Ascorbic acid, Uric acid	<200
Toluene, Phenol, 2-Nitrotoluene, 3-Nitrotoluene	20
4-Nitrophenol, 4-Nitrochlorobenzene, 2,4-Dichloro-1-nitrobenzene, 1,2-Dichloro-4-nitrobenzene	5
2-Nitrophenol	3
2,4-Dinitrophenol	1

*Because of the poor solubility of some potentially interfering species in PBS solution, ethanol was used as a cosolvent to increase their solubility.

Table 3. Determination of PA in waste and lake water.

Water type	Spiked concentration (μM)	Found concentration* (μM) (±SD)	Precision (RSD %)(N = 5)	Recovery %
Waste water	–	ND**	–	–
	70	73.92 (±0.03)	3.03	105.60
	200	207.99 (±0.02)	2.29	104.00
	400	401.23 (±0.02)	2.46	100.31
Lake water	–	ND**	–	–
	70	73.94 (±0.04)	3.70	105.63
	200	203.80 (±.03)	3.11	101.90
	400	401.16 (±0.03)	3.42	100.29

*The obtained values are the average of five determinations and the values in the parenthesis are the standard deviations.
**Not detected.

Different concentrations of PA were spiked in the BRB solution (0.1 M, pH = 6.0) which had been prepared by using the two natural water samples mentioned above. Then, standard addition method was used for PA determination in the real samples. As shown in Table 3, the satisfactory recoveries and precisions were obtained for determination of PA in the two real samples. These results show that the developed method is both accurate and precise.

4. Conclusion

In this work, PtNPs–rGO/GCE showed an excellent electrocatalytic behaviour towards PA reduction. Therefore, it was used as a new and simple electrochemical sensor for the quantification of PA in water samples. This sensor exhibited attractive features such as good selectivity, considerable sensitivity, ease of preparation, low-detection limit, wide linear range, satisfactory precision and recovery. Three well-defined irreversible reduction peaks were observed with significant potential differences. The most significant finding of the developed method was its satisfactory selectivity in determining PA in the presence of other NPhCs. In addition, satisfactory results were observed for the determination of PA in natural water samples. Hence, the proposed sensor will be applicable in analytical laboratories as a PA analysis method.

Acknowledgements

The authors wish to acknowledge the support of this work by Advanced Research Center of Elites, Tehran, Iran.

Disclosure statement

No potential conflict of interest was reported by the author.

Funding

This work was supported by the Advanced Research Center of Elites.

References

[1] M. Nipper, R. Scott Carr, J.M. Biedenbach, R.L. Hooten and K. Miller, Mar. Pollut. Bull. **50**, 1205 (2005). doi:10.1016/j.marpolbul.2005.04.019.
[2] J. Yinon, Trac Trends Anal. Chem. **21**, 292 (2002). doi:10.1016/S0165-9936(02)00408-9.
[3] J.F. Wyman, M.P. Serve, D.W. Hobson, L.H. Lee and D.E. Uddin, J. Toxicol. Environ. Health **37**, 313 (1992). doi:10.1080/15287399209531672.
[4] B. Roy, A.K. Bar, B. Gole and P.S. Mukherjee, J. Org. Chem. **78**, 1306 (2013). doi:10.1021/jo302585a.
[5] E. Bingham and B. Cohrssen, *Patty's Toxicology*, 6th ed. (Wiley, New York, 2012).
[6] V. Bhalla, S. Kaur, V. Vij and M. Kumar, Inorg. Chem. **52**, 4860 (2013). doi:10.1021/ic3023997.
[7] C. Beyer, U. Böhme, C. Pietzsch and G. Roewer, J. Organomet. Chem. **654**, 187 (2002). doi:10.1016/S0022-328X(02)01427-4.
[8] A. Kojlo, J. Karpinska, L. Kuzmicka, W. Misiuk, H. Puzanowska-Tarasiewicz and M. Tarasiewicz, J. Trace Microprobe Tech. **19**, 45 (2001). doi:10.1081/TMA-100001461.
[9] D. Tsikas, A. Wolf, A. Mitschke, F.M. Gutzki, W. Will and M. Bader, J. Chromatogr. B **878**, 2582 (2010). doi:10.1016/j.jchromb.2010.04.025.
[10] T.I.M.S. Lopes, A.O.S.S. Rangel, J.F.C. Lima and M.C.B.S.M. Montenegro, Anal. Chim. Acta **308**, 122 (1995). doi:10.1016/0003-2670(94)00598-G.
[11] M.V.S. Varma, A.M. Kaushal and S. Garg, J. Pharm. Biomed. Anal. **36**, 669 (2004). doi:10.1016/j.jpba.2004.07.044.
[12] A. Üzer, E. Erçağ and R. Apak, Anal. Chim. Acta **505**, 83 (2004). doi:10.1016/S0003-2670(03)00674-3.
[13] B. Agarwal, R. González-Méndez, M. Lanza, P. Sulzer, T.D. Märk, N. Thomas and C.A. Mayhew, J. Phys. Chem. A **118**, 8229 (2014). doi:10.1021/jp5010192.
[14] O.M. Ivanova, V.A. Raks and V.N. Zaitsev, J. Water Chem. Technol. **36**, 273 (2014). doi:10.3103/S1063455X14060034.
[15] O. Cascio, M. Trettene, F. Bortolotti, G. Milana and F. Tagliaro, Electrophoresis **25**, 1543 (2004). doi:10.1002/elps.200305883.
[16] M. Burdel, J. Šandrejová, I.S. Balogh, A. Vishnikin, V. Andruch and J. Sep, Sci. **36**, 932 (2013).
[17] V. Vyskočil, T. Navrátil, A. Daňhel, J. Dědík, Z. Krejčová, L. Škvorová, J. Tvrdíková and J. Barek, Electroanalysis **23**, 129 (2011). doi:10.1002/elan.201000428.
[18] O. El Tall, D. Beh, N. Jaffrezic-Renault and O. Vittori, Int. J. Environ. Anal. Chem. **90**, 40 (2010). doi:10.1080/03067310902871265.
[19] J. Huang, L. Wang, C. Shi, Y. Dai, C. Gu and J. Liu, Sens. Actuators B: Chem. **196**, 567 (2014). doi:10.1016/j.snb.2014.02.050.
[20] K. Giribabu, S.Y. Oh, R. Suresh, S.P. Kumar, R. Manigandan, S. Munusamy, G. Gnanamoorthy, J. Y. Kim, Y.S. Huh and V. Narayanan, Microchim. Acta **183**, 2421 (2016). doi:10.1007/s00604-016-1883-7.
[21] M. Jacobsen, H. Duwensee, F. Wachholz, M. Adamovski and G.U. Flechsig, Electroanalysis **22**, 1483 (2010). doi:10.1002/elan.200900486.
[22] A. Safavi, R. Ahmadi and F.A. Mahyari, Amino Acids **46**, 1079 (2014). doi:10.1007/s00726-014-1668-4.
[23] D. Nie, Y. Liang, T. Zhou, Q. Sun, G. Shi and L. Jin, Int. J. Environ. Anal. Chem. **92**, 832 (2012). doi:10.1080/03067319.2010.520124.
[24] J. Wang, D.F. Thomas and A. Chen, Anal. Chem. **80**, 997 (2008). doi:10.1021/ac701790z.
[25] Y. Liu, X. Dong and P. Chen, Chem. Soc. Rev. **41**, 2283 (2012). doi:10.1039/C1CS15270J.
[26] A. Safavi, R. Ahmadi, F.A. Mahyari, M. Tohidi and B. Sensors Actuators, Chem. **207**, 668 (2015).
[27] D.A. Dikin, S. Stankovich, E.J. Zimney, R.D. Piner, G.H.B. Dommett, G. Evmenenko, S.T. Nguyen and R.S. Ruoff, Nature **448**, 457 (2007). doi:10.1038/nature06016.
[28] G.M. Scheuermann, L. Rumi, P. Steurer, W. Bannwarth and R. Mülhaupt, J. Am. Chem. Soc. **131**, 8262 (2009). doi:10.1021/ja901105a.
[29] A. Safavi, F.A. Mahyari and M. Tohidi, Mater. Res. Bull. **48**, 3399 (2013). doi:10.1016/j.materresbull.2013.05.013.

[30] Y. Qin, L. Chao, J. Yuan, Y. Liu, F. Chu, Y. Kong, Y. Tao and M. Liu, Chem. Commun. **52**, 382 (2016). doi:10.1039/C5CC07482G.
[31] Z. Yang, Y. Cao, J. Li, Z. Jian, Y. Zhang and X. Hu, Anal. Chim. Acta **871**, 35 (2015). doi:10.1016/j.aca.2015.02.029.
[32] E. Er, H. Çelikkan, N. Erk and B. Sensors Actuators, Chem. **238**, 779 (2017).
[33] S. Palanisamy, H.F. Lee, S.M. Chen and B. Thirumalraj, RSC Adv. **5**, 105567 (2015). doi:10.1039/C5RA20512C.
[34] M. Raj, P. Gupta, N. Thapliyal and R.N. Goyal, Electroanalysis **28**, 1 (2016). doi:10.1002/elan.201680101.
[35] P. Pang, H. Li, Y. Liu, Y. Zhang, L. Feng, H. Wang, Z. Wu and W. Yang, Anal. Methods **7**, 3581 (2015). doi:10.1039/C5AY00353A.
[36] Y. Chen, X. Zhang, P. Yu and Y. Ma, Chem. Commun. 2009, 4527. doi:10.1039/b907723e.
[37] X. Wang, X. Wen, Z. Liu, T. Tan, Y. Yuan and P. Zhang, Nanotechnology **23**, 485604 (2012). doi:10.1088/0957-4484/23/48/485604.
[38] O. Akhavan, E. Ghaderi, S. Aghayee, Y. Fereydooni and A. Talebi, J. Mater. Chem. **22**, 13773 (2012). doi:10.1039/c2jm31396k.
[39] B. Zahed and H. Hosseini-Monfared, Appl. Surf. Sci. **328**, 536 (2015). doi:10.1016/j.apsusc.2014.12.078.
[40] G.H. Moon, D.H. Kim, H.I. Kim, A.D. Bokare and W. Choi, Environ. Sci. Technol. Lett. **1**, 185 (2014). doi:10.1021/ez5000012.
[41] J.R.C. Junqueira, W.R. De Araujo, M.O. Salles and T.R.L.C. Paixão, Talanta **104**, 162 (2013). doi:10.1016/j.talanta.2012.11.036.
[42] H.X. Zhang, A.M. Cao, J.S. Hu, L.J. Wan and S.T. Lee, Anal. Chem. **78**, 1967 (2006). doi:10.1021/ac051826s.
[43] I. Grigoriants, B. Markovsky, R. Persky, I. Perelshtein, A. Gedanken, D. Aurbach, B. Filanovsky, T. Bourenko and I. Felner, Electrochim. Acta **54**, 690 (2008). doi:10.1016/j.electacta.2008.07.005.
[44] I. Tredici, D. Merli, F. Zavarise and A. Profumo, J. Electroanal. Chem. **645**, 22 (2010). doi:10.1016/j.jelechem.2010.03.036.
[45] B. Filanovsky, B. Markovsky, T. Bourenko, N. Perkas, R. Persky, A. Gedanken and D. Aurbach, Adv. Funct. Mater. **17**, 1487 (2007). doi:10.1002/adfm.200600714.
[46] V.V. Singh, A.K. Nigam, S.S. Yadav, B.K. Tripathi, A. Srivastava, M. Boopathi, B. Singh and B. Sensors Actuators, Chem. **188**, 1218 (2013).
[47] M. Riskin, R. Tel-Vered, T. Bourenko, E. Granot and I. Willner, J. Am. Chem. Soc. **130**, 9726 (2008). doi:10.1021/ja711278c.
[48] T.W. Chen, Z.H. Sheng, K. Wang, F.B. Wang and X.H. Xia, Chem. Asian J. **6**, 1210 (2011). doi:10.1002/asia.201000836.
[49] H. Hosseini, M. Mahyari, A. Bagheri and A. Shaabani, Biosens. Bioelectron. **52**, 136 (2014). doi:10.1016/j.bios.2013.08.041.
[50] H. Hosseini, H. Ahmar, A. Dehghani, A. Bagheri, A.R. Fakhari and M.M. Amini, Electrochim. Acta **88**, 301 (2013). doi:10.1016/j.electacta.2012.10.064.
[51] A. Bagheri and H. Hosseini, Bioelectrochem. **88**, 164 (2012). doi:10.1016/j.bioelechem.2012.03.007.
[52] Y. Ni, L. Wang and S. Kokot, Anal. Chim. Acta **431**, 101 (2001). doi:10.1016/S0003-2670(00)01319-2.